Macromolecules
ARTICLE

Macromolecules **2009**, *42*, 6245–6252 **6245**
DOI: 10.1021/ma901013q

SANS and SLS Studies on Tetra-Arm PEG Gels in As-Prepared and Swollen States

Takuro Matsunaga,[†,§] Takamasa Sakai,[‡,§] Yuki Akagi,[‡] Ung-il Chung,[‡] and Mitsuhiro Shibayama*[,†]

[†]*The Institute for Solid State Physics, The University of Tokyo 5-1-5 Kashiwanoha, Kashiwa, Chiba 277-8581, Japan, and* [‡]*Department of Bioengineering, School of Engineering, The University of Tokyo 7-3-1 Hongo, Bunkyo-ku, Tokyo 113-8656, Japan.* [§]*Cofirst author. These authors contributed equally to the work.*

Received May 9, 2009; Revised Manuscript Received July 9, 2009

ABSTRACT: A series of model networks consisting of polyethylene glycol (PEG), tetra-PEG gels, have been prepared and their structure and dynamics have been investigated by small-angle neutron scattering (SANS) and static light scattering (SLS). The Tetra-PEG gels were prepared by cross-end coupling of two types of tetra-arm PEG macromers with molecular weights, M_w, of (5 to 40) $\times 10^3$ g/mol. In the SANS regime, the structure factors of both as-prepared and swollen gels can be represented by Ornstein−Zernike-type scattering functions and superimposed to single master curves with the reduced variables, ξq and $I(q)/\phi_0\xi^2$, irrespective of the molecular weight of tetra-PEG, where q, ξ, $I(q)$, and ϕ_0 are the magnitude of the scattering vector, the correlation length, the scattering intensity, and the polymer volume fraction at preparation, respectively. In the SLS regime, however, a power-law-type upturn was observed, indicating the presence of PEG chain clusters. Interestingly, these inhomogeneities disappear by swelling. It is concluded that Tetra-PEG gels can be an "ideal polymer network" with a self-similar structure with respect to M_w without significant entanglements and/or defects. This explains why Tetra-PEG gels have high mechanical strength as reported elsewhere (*Macromolecules* **2008**, *41*, 5379).

1. Introduction

It is well known that polymer gels have inhomogeneous structures.[1−6] Because these inhomogeneous structures are only "topologically frozen", a polymer gel in a solvent is an open system and is able to obey thermodynamics.[7] This is why a gel can change its volume depending on its environment and reach thermodynamic equilibrium.[8,9] Inhomogeneous structures in polymer gels are ascribed to an introduction of cross-links to a polymeric system, which fixes the topological architecture of the system. These inhomogeneities are often characterized by an upturn in the scattering intensity at low q region in small-angle neutron scattering (SANS)[10] or a speckle pattern in laser light scattering,[11,12] where q is the magnitude of the scattering vector. There are various types of inhomogeneities, such as spatial, topological, connectivity, and mobility inhomogeneities, as classified by one of the authors.[13] A large number of studies on the structural characterization of polymer gels have been carried out by using these properties.[6]

Recently, however, some exceptions are reported. For example, polymer gels that do not exhibit nonergodicity are reported by Wu.[14] They demonstrated that inhomogeneities in an assembly of microgels were strongly suppressed if individual swollen microgels were closely packed to each other. On the basis of this experimental evidence, they concluded that static nonergodic behavior originated from large "voids" formed during sol−gel transition in the polymerization process. It should be noted, however, that the gels reported by Wu were microgels, and the absence of inhomogeneities was exclusively observed in the jam-packed state where the concentration fluctuations are strongly suppressed. Here the "voids" refer to the polymer-poor region in a gel. Inhomogeneities are also found even in physical gels, which spontaneously tune their network by "detachable" cross-links so as to minimize the free energy of entropy elasticity.[15,16] Here a frozen component in the concentration fluctuations starts to appear as soon as a sol−gel transition occurs. Therefore, in general, polymer gels inherently possess inhomogeneities because of the presence of cross-links.

Because the physical properties of gels, such as mechanical properties and optical properties, strongly depend on the structure, it is extremely important to clarify the relationship between structure and mechanical properties. The understanding of cross-link inhomogeneities is vital from both scientific and engineering points of view because they affect the physical properties of the network polymer, such as mechanical and optical properties.[17] There has been a desire to prepare an "ideal" polymer network that is free from defects.[18] One of the theoretically promising methods to prepare a model network was end-coupling of telechelic polymer having a sharp molecular weight distribution by multifunctional cross-linker.[19−23] However, there has been no success in preparing defect-free networks so far.[24−26] No matter how precisely one controlled the architecture, the obtained "model network" had strong forward scattering at low q region and or exhibited double-shoulder scattering curves. For example, Mendes et al. classified gel structures to (I) the one-correlation length gels, (II) the soft-order gels that have a scattering maximum, and (III) the two-correlation length gels.[25]

Sakai et al. developed a novel class of hydrogels by cross-end coupling of two types of tetra-arm polyethylene glycol (PEG) chains.[27] These gels, hereafter called Tetra-PEG gels, have various advantages, namely, high mechanical strength and toughness, easy preparation, and biocompatibility. Interestingly, it was found that Tetra-PEG gels were free from inhomogeneities

*To whom correspondence should be addressed. E-mail: shibayama@issp.u-tokyo.ac.jp.

© 2009 American Chemical Society

Published on Web 07/21/2009

characterized by the above-mentioned upturn behavior at low q regions ($q < 0.01$ Å^{-1}) in SANS.[28] We then concluded that the extraordinary toughness of Tetra-PEG gels was ascribed to a "perfect" and "ideal" network such as a diamondlike tetrahedral structure.[28] In this article, we discuss the structure of Tetra-PEG gels in more detail with the scattering intensity data in a wide q range covering not only the SANS ($0.003 \le q \le 0.2$ Å^{-1}) but also the light scattering (LS) regime ($0.0008 \le q \le 0.002$ Å^{-1}).

2. Theoretical Background

2.1. Scattering Functions for Multiarm Polymer Chains. The form factor of multiarm star polymer chains, $P_{\mathrm{star}}(q)$, is given by[29,30]

$$P_{\mathrm{star}}(q) = \frac{2Z}{fu^2}\left\{u - [1 - \exp(-u)] + \frac{f-1}{2}[1 - \exp(-u)]^2\right\} \tag{1}$$

Here f is the number of arms of the star polymer, Z is the degree of polymerization, and $u \equiv Za^2q^2/6$ with a being the segment length. Equation 1 is a "Debye function" for the f-arm polymer chain. The interpolymer interaction can be taken into consideration in terms of the Flory−Huggins interaction parameter, χ, and the scattering intensity is given by

$$I(q) = \frac{(\Delta\rho)^2}{N_{\mathrm{A}}}\frac{V_2\phi P_{\mathrm{star}}(q)}{1 + (1-2\chi)\left(\frac{V_2}{V_1}\right)\phi P_{\mathrm{star}}(q)} \tag{2}$$

Here N_{A} is Avogadro's number and ϕ is the volume fraction of the solute. V_1 and V_2 are the molar volumes of the solvent and the monomeric unit of the solute, respectively. $(\Delta\rho)^2$ is the scattering length density difference square between polymer 2 and solvent 1.

$$(\Delta\rho)^2 = (\rho_2 - \rho_1)^2 = \left[\left(\frac{b_2}{\tilde{V}_2}\right) - \left(\frac{b_1}{\tilde{V}_1}\right)\right]^2 \tag{3}$$

where b_i and $\tilde{V}_i$ ($\equiv V_i/N_{\mathrm{A}}$) are the scattering length and the volume of the solvent ($i = 1$) and the monomeric unit of component ($i = 2$).

2.2. Scattering Functions of Polymer Gels. According to de Gennes,[31] the scattering intensity function of polymer gels in swelling equilibrium is the same as that of polymer solutions at the same concentration and is given by

$$I(q) = \frac{(\Delta\rho)^2 RT\phi^2}{N_{\mathrm{A}}M_{\mathrm{os}}}\frac{1}{1 + \xi^2q^2} \tag{4}$$

Here ξ is the correlation length of the network, R is the gas constant, and T is the absolute temperature. M_{os} is the osmotic modulus of the gel given by[9]

$$M_{\mathrm{os}} = \frac{RT\phi^2}{V_1}\left(\frac{1}{1-\phi} - 2\chi\right) + \nu_{\mathrm{e}}RT\left[\frac{1}{2}\left(\frac{\phi}{\phi_0}\right) + \left(\frac{\phi}{\phi_0}\right)^{1/3}\right] \tag{5}$$

where ν_{e} is the number density of the effective elastic chains in the network. In principle, the scattering function can be represented by the so-called Ornstein−Zernike function,[32] that is, eq 4. However, it is known that scattering intensity functions of gels have significant forward scattering at low q region due to cross-linking inhomogeneities. As a result, by adding an extra term, eq 4 is modified to[28]

$$I(q) = \frac{(\Delta\rho)^2 RT\phi^2}{N_{\mathrm{A}}M_{\mathrm{os}}}\left[\frac{1}{1 + \xi^2q^2} + \frac{A_{\mathrm{inhom}}}{(1 + \Xi^2q^2)^2}\right] \tag{6}$$

The extra term A_{inhom} is dependent on the chemistry of gel preparation because it represents how the component polymer chains are topologically frozen by cross-linking.

3. Experimental Section

3.1. Sample Preparation. Tetra-amine-terminated PEG (TAPEG) and tetra-NHS-glutarate-terminated PEG (TNPEG) were prepared from tetrahydroxyl-terminated PEG (THPEG) having equal arm lengths. Here NHS represents *N*-hydroxysuccinimide. The details of TAPEG and TNPEG preparation are reported elsewhere.[27] The molecular weights (M_{w}) of TAPEG and TNPEG were matched to each other, and four sets of samples having different M_{w} values were prepared, that is, $M_{\mathrm{w}} = 5k$, $10k$, $20k$, and $40k$ g/mol. The sample code is given by the M_{w}, for example, Tetra-PEG-5k being Tetra-PEG with $M_{\mathrm{w}} = 5 \times 10^3$. The activity of the functional group was estimated using NMR. Tetra-PEG gels were synthesized as follows. Equal amounts of TAPEG and TNPEG (5−160 mg/mL) were dissolved in phosphate buffer (pH 7.4) and phosphate−citric acid buffer (pH5.8), respectively. To obtain coherent neutron scattering from the polymers, these buffer solutions were prepared with deuterated water. To control the reaction rate, the ionic strengths of buffers were chosen to be 25 mM for lower macromer concentrations (5−100 mg/mL) and 75 mM for higher macromer concentrations (110−160 mg/mL) for Tetra-PEG-10k. The ionic strengths of buffers were chosen to be 50 mM for lower macromer concentrations (5−100 mg/mL) and 100 mM for higher macromer concentrations (110−160 mg/mL) for Tetra-PEG-5k, -20k, and -40k. Two solutions were mixed, and the resulting solution was poured into the mold. At least 12 h were spent for the completion of the reaction before the following experiments.

3.2. Small-Angle Neutron Scattering. SANS experiments were carried out on a 2D SANS instrument, SANS-U,[33,34] at the University of Tokyo, located at JRR-3 Research Rector, Japan Atomic Energy Agency, Tokai, Ibaraki, Japan. A monochromated cold neutron beam with an average neutron wavelength of 7.00 Å and 10% wavelength distribution was irradiated to the samples. The scattered neutrons were counted with a 2D position detector (Ordela 2660N, Oak Ridge). The sample-to-detector distances were chosen to be 1 and 4 m for macromer (TAPEG) measurements and 2 and 8 m for Tetra-PEG-gel measurements. After necessary corrections for open beam scattering, transmission, and detector inhomogeneities, the corrected scattering intensity functions were normalized to the absolute intensity scale with a polyethylene secondary standard. The details of the instrument are reported elsewhere.[33,34] Incoherent scattering subtraction was made with the method reported by Shibayama et al.[35a,35b]

3.3. Static Light Scattering. SLS measurements were performed by a static/dynamic compact goniometer (DLS/SLS-5000), ALV, Langen, Germany. A He−Ne laser with a power of 22 mW emitting a polarized light at $\lambda = 6328$ Å was used as the incident beam. SLS intensity functions were taken at 20 °C at scattering angles of 30 to 150°.

4. Results and Discussion

4.1. Macromer Solutions. Figure 1 shows the scattering intensity curves of (a) TAPEG-5k, (b) TAPEG-10k, (c) TAPEG-20k, and (d) TAPEG-40k macromer solutions in the as-prepared state with various concentrations, ϕ (= ϕ_0). The solid lines show the curve fits with eq 2, that is, the scattering function for tetra-arm polymer chains. All observed SANS functions were well-represented by eq 2. It should be noted that the interaction parameter, χ, has to be varied from 0.495 (TAPEG-5k) to 0.465 (TAPEG-40k) to reproduce the observed SANS intensity functions with eq 2. The molecular weight dependence of the interaction parameter χ is shown in Figure 2, which seems to be a decreasing

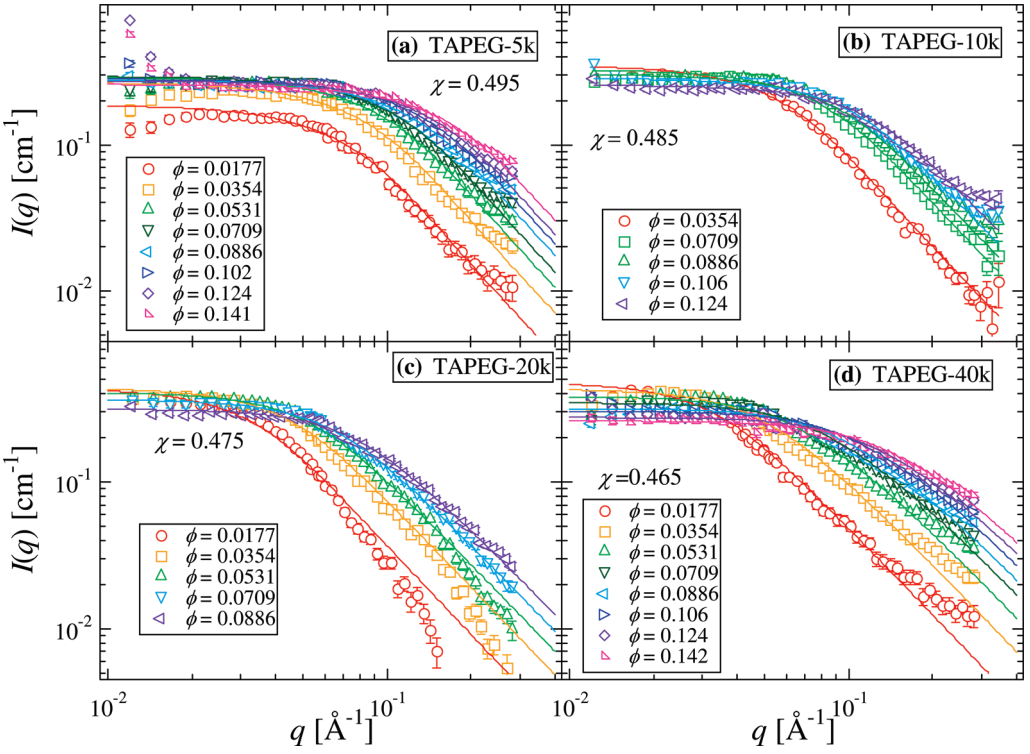

Figure 1. Scattering intensity curves of TAPEG macromer solutions, (a) TAPEG-5k, (b) TAPEG-10k, (c) TAPEG-20k, and (d) TAPEG-40k.

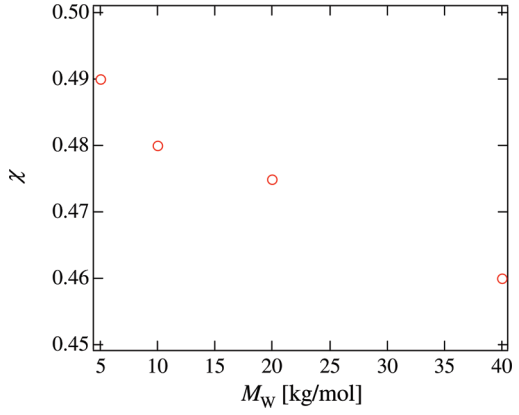

Figure 2. Molecular weight dependence of the apparent interaction parameter χ.

function of M_w. The reason for the M_w dependence may be the presence of the arm-end,[27] and the chain-end effect becomes insignificant with increasing M_w. As a matter of fact, the value of χ approaches the value of linear PEG chains[36] ($\chi = 0.43$ at $T = 20$ °C) by increasing M_w.

Figure 3 shows the M_w and concentration dependence of the radius of gyration, R_g, of TAPEG. R_g seems to be a decreasing function of the initial polymer fraction, ϕ_0, as well as of M_w. The inset shows that R_g is roughly given by $R_g \approx \phi_0^{-1/3}$, indicating that a simple contraction occurs in Tetra-PEG chains as a function of ϕ_0. This exponent indicates that the Tetra-PEG chains behave as compressive elastic balls that are dependent on the concentration, and no interpenetration occurs even at $\phi_0 > \phi_0^*$, where ϕ_0^* is the overlap concentration. The absence of interpenetration may be due to the presence of a large number of end groups, as discussed in the previous paper.[28] However, regarding M_w dependence, the plots of R_g versus ϕ_0 in the inset do not seem to be superimposed by shifting with an equal gap, although the

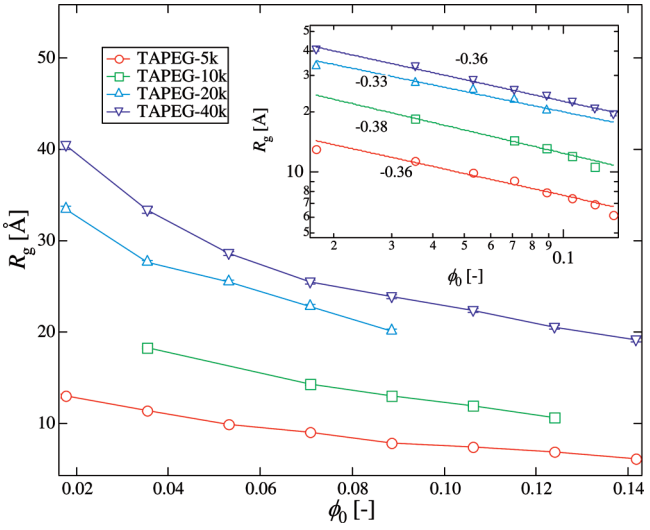

Figure 3. Polymer concentration dependence of the radius of gyration, R_g, of TAPEGs having various M_w values. The inset shows the log−log plots.

M_w of the TAPEGs are in a series of two folds (i.e., 5k, 10k, 20k, and 40k). Therefore, there is a strong deviation from a power law, that is, $R_g \approx M_w^{\alpha}$ with $\alpha = 1/2$ (Θ-solvent) or 3/5 (good solvent). Figure 4 shows the M_w dependence of R_g for the case of $\phi_0 = 0.0709$. The dashed and chain lines are calculated values by assuming $R_g \approx M_w^{\alpha}$ with $\alpha = 1/2$ and 3/5, respectively. Interestingly, a relation $R_g \approx M_w^{1/2}$ is obtained for TAPEG-5k and TAPEG-40k, although a significant positive deviation is seen for TAPEG-10k and TAPEG-20k. The reason is not clear in this stage.

4.2. Tetra-PEG Gels in As-Prepared State. Figure 5 shows SANS curves of as-prepared gels for (a) Tetra-PEG-5k gels, (b) Tetra-PEG-10k gels, (c) Tetra-PEG-20k gels, and (d) Tetra-PEG-40k gels. Note that these subfigures correspond

to those of Figure 1. The solid lines are the fits with eq 4, that is, the Ornstein−Zernike (OZ) function. In the case of as-prepared Tetra-PEG-5k gel, a strong upturn in $I(q)$ for $q \leq 0.01$ Å^{-1} is observed for $\phi_0 \geq 0.0531$, and a fitting with eq 4 is poor. However, for larger q, each $I(q)$ can be fitted with an OZ function. Unlike the case of Tetra-PEG-5k gels, no significant upturn in $I(q)$ is found at low q region in Tetra-PEG-10, -20k, and -40k in this q region. It should be noted here the following: Polymer gels usually exhibit a strong upturn in low q region because of the presence of inhomogeneities.[5,6] Even in the case of "ideal polymer networks" made by end-linking of telechelic polymer chains, significant inhomogeneities are reported.[25,26]

Figure 6 shows the concentration dependence of the correlation length, ξ, for Tetra-PEG gels with various M_w values. Surprisingly, the larger M_w is, the smaller ξ is. If ξ represents the mesh size formed by cross-end-coupling of TAPEG and TNPEG, then ξ should increase with M_w by a power of either 1/2 (Θ solvent) or 3/5 (good solvent). The experimental results, however, show the opposite behavior. The concentration dependence of ξ is also quite different from that of the macromers. Although ξ seems to be well represented by a power-law function of ϕ_0 for each set of Tetra-PEG, as shown in the inset, the exponents are much larger than −3/4 expected for a semidilute solution in a good solvent as well as for a gel in swelling equilibrium.[31] These exponents seem to decrease as M_w increases and approach the value, that is, −3/4. As a matter of fact, Tetra-PEG-40k gels show $\xi \approx \phi_0^{-0.78}$, of which the exponent is close enough to −3/4. (See the inset of Figure 6.) Therefore, it is conjectured that the observed ξ for Tetra-PEG-40k gels represents the size of the "mesh" of the polymer network. However, those for 5k, 10k, and 20k may represent additional concentration fluctuations, of which correlation lengths are much larger than the mesh size. This is probably due to the formation of an imperfect polymer network, as schematically shown in Figure 7. That is, if an arm chain is not long enough, then the arm chain is too rigid to undergo the cross-end-coupling reaction between TAPEG and

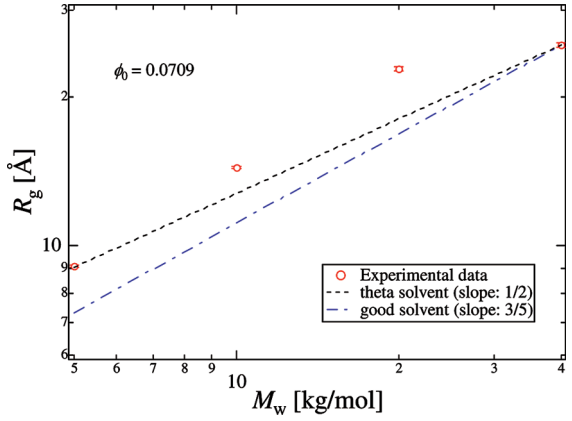

Figure 4. M_w dependence of R_g for $\phi_0 = 0.0709$. The dashed and chain lines denote calculated values by assuming $R_g \approx M_w^{\alpha}$ with $\alpha = 1/2$ and 3/5, respectively.

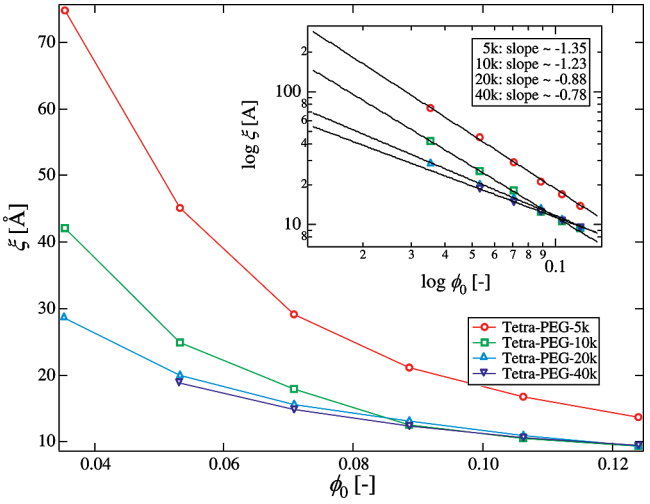

Figure 6. Concentration dependence of the correlation length, ξ, for Tetra-PEG gels with macromer molecular weights of 5k, 10k, 20k, and 40k.

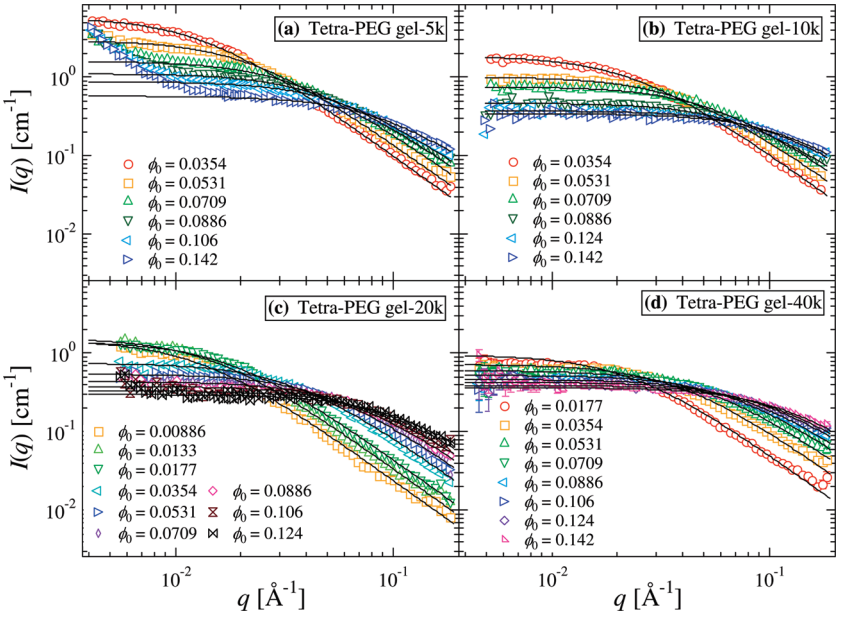

Figure 5. SANS curves of as-prepared gels for (a) Tetra-PEG-5k, (b) -10k, (c) -20k, and (d) -40k. The solid lines denote the results of curve fit with OZ functions.

TNPEG with a high yield. If this is the case, then a large number of network defects are formed, leading to an observation of a larger mesh size characterized by the correlation length, ξ. The yield of cross-end coupling is expected to increase by increasing the initial polymer concentration, leading to a stronger concentration dependence of ξ. This may be why the exponent is much larger than that expected for the polymer network in a good solvent. However, these structural and kinetic constraints are suppressed by increasing M_w, leading to the recovery of the expected exponent.

4.3. Swollen Gels in Swelling Equilibrium. Figure 8 shows a series of SANS intensity functions for Tetra-PEG gels in swelling equilibrium for (a) Tetra-PEG gel-5k, (b) -10k, (c) -20k, and (d) -40k. As shown in these Figures, $I(q)$ values for the swollen gels are satisfactorily fitted with OZ functions irrespective of ϕ. Here note that ϕ is the polymer volume fraction at swelling equilibrium, which is different from the polymer volume fraction at preparation, ϕ_0. As shown in these Figures, cross-linking inhomogeneities seem to disappear by swelling, which is opposite to the case of randomly cross-linked conventional gels (statistical gels).[37−42] Note that in the case of conventional gels, cross-linking inhomogeneities are not explicit in as-prepared gels because cross-links are introduced so as to minimize the free energy. However, cross-linking inhomogeneities become explicit because of inhomogeneous swelling according to the difference in the local cross-link density, as was explained by Bastide and Leibler.[37] Even in the case of statistical gels made by end-linking, swollen gels exhibit an upturn in SANS.[26] Therefore, the absence of an upturn in the SANS intensity functions observed in Tetra-PEG gels is quite unusual. Another interesting feature of Tetra-PEG gels is that the SANS intensity functions become ϕ-independent by increasing M_n. The reason for this unique behavior will be discussed later.

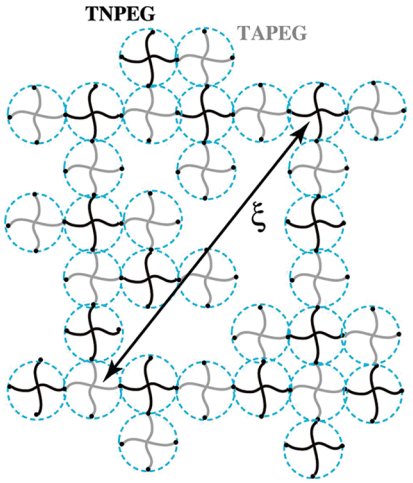

Figure 7. Schematical representation of the structure of Tetra-PEG-5k gels. Because of the imperfect cross-end-coupling reaction, large voids are formed, which are characterized by ξ.

Figure 9 shows ξ versus ϕ plots for swollen gels for (a) Tetra-PEG-5k, (b) -10k, (c) -20k, and (d) -40k (solid symbols with solid lines) as well as ξ versus ϕ_0 plots for as-prepared gels (open symbols and broken lines). Various interesting features can be extracted from this Figure. First, ξ increases by swelling (i.e., the values of ξ move left and upward by changing ϕ_0 to ϕ). Second, different from the case of as-prepared gels (Figure 6), no clear relationship between ξ and ϕ is found in the swollen gels. Third, the ϕ dependence of ξ becomes smaller by increasing M_w. For example, in the case of Tetra-PEG-40k, ξ and ϕ are collapsing into a small region of $\xi \approx 60$ Å and $0.01 < \phi < 0.02$ independent of ϕ_0. This tendency seems reasonable because a unique set of values of ξ and ϕ is expected to exist in a gel at swelling equilibrium, that is, (ξ_{eq}, ϕ_{eq}), for a network with a given set of M_w and χ. This tendency weakens as M_w decreases. For example, in the case of Tetra-PEG-5k, ξ changed little with swelling and ξ scales with $\phi^{-1.01}$. Therefore, a unique set of values of ξ and ϕ does not exist for Tetra-PEG-5k, and hence it is concluded that Tetra-PEG-40k gel is closer to an ideal network than other gels with lower M_w values.

Figure 10 schematically shows as-prepared Tetra-PEG-40k gels as a function of ϕ_0 and those in swelling equilibrium at the polymer volume fraction ϕ. In the case of as-prepared gels, the characteristic size of the network scales with ϕ_0^{γ}, where the exponent γ is close to $-3/4$. (See Figure 9.) When

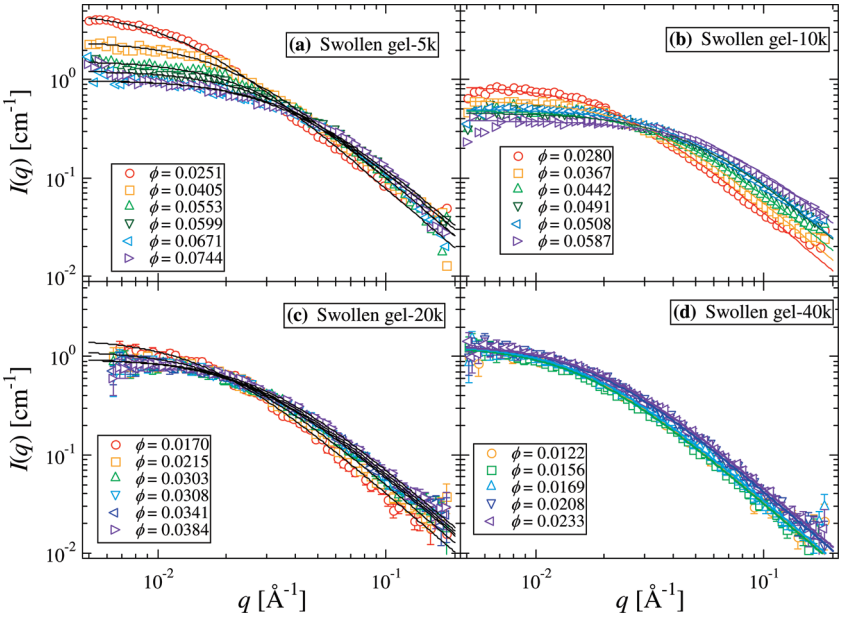

Figure 8. Series of SANS intensity functions for Tetra-PEG gels in swelling equilibrium for (a) Tetra-PEG gel-5k, (b) -10k, (c) -20k, and (d) -40k. The solid lines denote the results of curve fit with OZ functions.

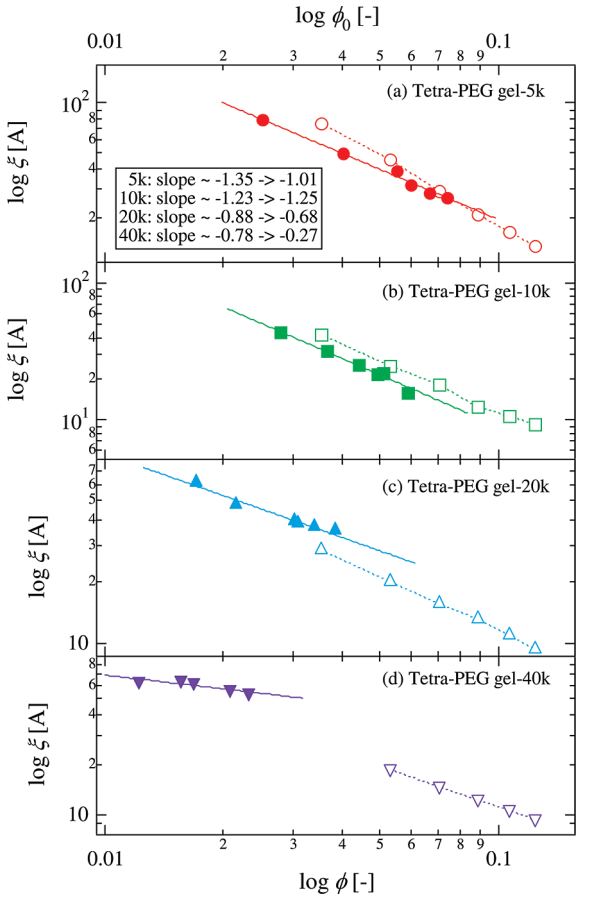

Figure 9. Concentration dependence of ξ of swollen gels for Tetra-PEG gel-5k, -10k, -20k, and -40k (solid symbols with solid lines) as well as those of as-prepared gels (open symbols and broken lines).

the gels are swollen in water, they reach a unique swollen state depending on their molecular weights, as shown schematically in the bottom of Figure 10. The presence of a unique swollen state independent of ϕ_0 suggests that the cross-linking reaction occurs exclusively at the surface of Tetra-PEG macromers and no entanglement formation takes place. Therefore, it is concluded that the cross-end-coupling employed in this system is an effective method to prepare an ideal network without defects or trapped entanglements.

4.4. Master Curves. In the discussion of Figure 5, it was pointed out that a strong upturn was observed at the low q region for Tetra-PEG-5k gel. To elucidate this anomaly in the low q region ($0.003 \leq q \leq 0.02$ Å^{-1}), we carried out SLS in the region of $0.0008 \leq q \leq 0.002$ Å^{-1}. Figure 11a shows the result of SANS as well as SLS experiments. Although there is a small missing region between SANS and SLS data (marked by the dashed line), both sets of scattering intensity data seem to be smoothly connected to each other, and a master curve is obtained. Note that the SLS data are shifted vertically so as to be connected to the corresponding SANS data. More interestingly, by scaling $I(q)/\phi_0\xi^2$ and ξq, all scattering intensity curves fall onto a single master curve, as shown in Figure 11b. Similar behaviors were also observed in all Tetra-PEG gels. This strongly indicates that Tetra-PEG gels have a self-similar structure with respect to the polymer concentration at preparation, ϕ_0. This Figure also shows that Tetra-PEG gels have two characteristic length scales, that is, the correlation length, ξ, and the characteristic length of inhomogeneities, Ξ, given by eq 6. Now, let us discuss the origin of the inhomogeneities characterized by Ξ.

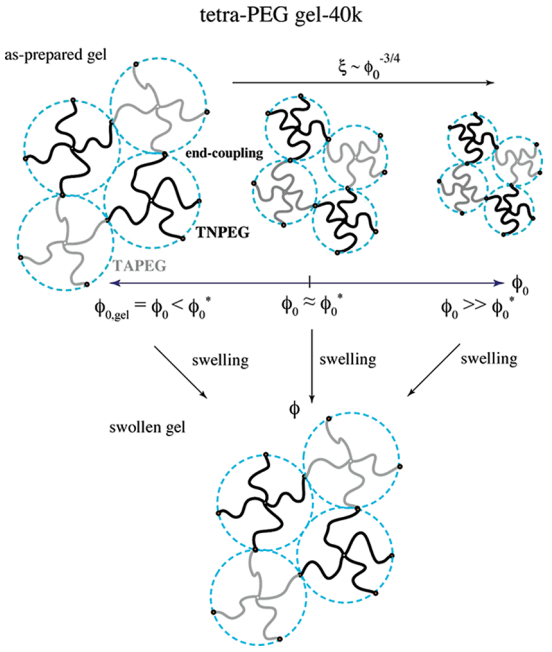

Figure 10. Schematic representation showing the change of network size as a function of ϕ_0 and of ϕ.

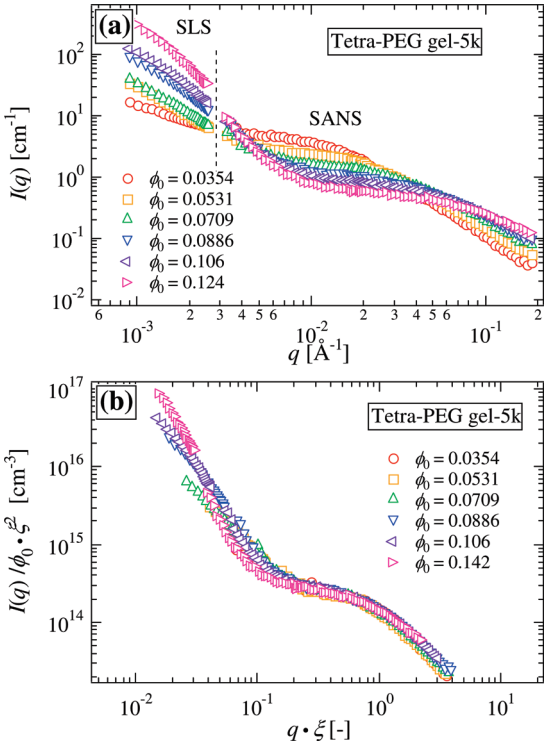

Figure 11. (a) SANS as well as SLS intensity functions for Tetra-PEG gel-5k prepared at various concentrations, ϕ_0. The missing q region is indicated by the vertical dashed line. (b) Scaled plots, $I(q)/\phi_0\xi^2$ and ξq.

It is more interesting to compare the master curves in the scattering intensity functions of Tetra-PEG gels having different M_w values. Figure 12 shows the plots of the master curves obtained for Tetra-PEG gel-5k (○), -10k (□), -20k (△), and -40k (◇). The curves denoted by crosses indicate the scattering intensity function of linear PEG chains ($M_w = 102 \times 10^3$ at 10 °C) reported by Hammouda.[43] Surprisingly enough, the SANS function for the linear PEG chains is also nicely superimposed to the master curve by employing the reduced

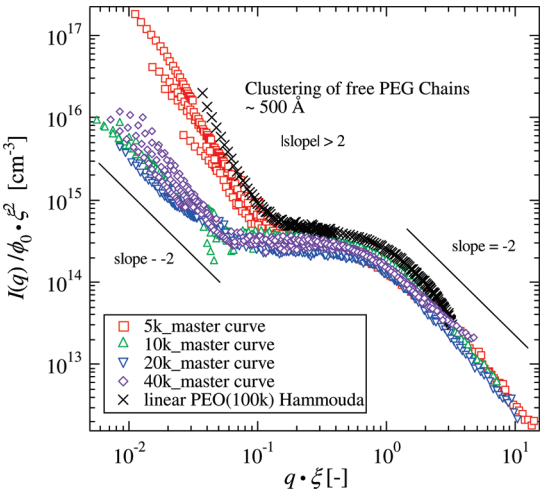

Figure 12. Scaled plots, $I(q)/\phi_0\ \xi^2$ and ξq, for Tetra-PEG gel-5k (○), -10k (□), -20k (△), and -40k (◇). Crosses indicate the reduced scattering intensity function for linear PEG chains (M_n = 100k) in water.

variables, as shown in Figure 12. It is reported that this upturn corresponds to clustering of PEG chains in water with a typical size of 500 Å, and the major reason for clustering is the presence of hydrophobic end groups, such as $-OCH_3$. It is of particular interest that the behavior of the linear PEG is quite similar to that of the Tetra-PEG-5k gel. This suggests that Tetra-PEG-5k gel has a clustered structure similar to that of linear PEG chains in water. This is probably due to clustering of arm PEG chains with unreacted end group. It is noted that the presence of such a clustered (or aggregated) structure is typical in PEG aqueous solutions.[44–46] Figure 12 indicates that this clustered structure seems to be suppressed by increasing M_w.

Hammouda et al. proposed two kinds of scattering functions different in the cluster term, that is, the Debye–Bueche-type squared-Lorentz function[43] and a power-law functions[45]

$$I(q) = \frac{A}{(1+\Xi^2 q^2)^2} + \frac{B}{1+\xi^2 q^2} \quad \text{(Debye–Bueche function)} \tag{7}$$

and

$$I(q) = A' q^{-\beta} + \frac{B}{1+\xi^2 q^2} \quad \text{(power-law function)} \tag{8}$$

where A, B, and A' are numerical factors, and β is a scattering exponent. Note that the scattering form of eq 7 is exactly the same as that of eq 6 and is employed by many researchers including the authors.[6,7,47,48] This means that there exists a two-phase structure that has a sharp boundary characterized by the so-called Porod law ($I(q) \approx q^{-4}$). However, eq 8 suggests the presence of a fractal structure characterized by mass fractal, $D = \beta$.[49–51] The scattering exponent at the low q region in Figure 11b is close to -2. Therefore, the hypothesis of the presence of a two-phase structure with a sharp boundary does not seem to be applicable to Tetra-PEG gels. This exponent (-2) revealed in Tetra-PEG gels for $M_w \geq 10$k may indicate that Tetra-PEG gels have two correlation lengths ξ and Ξ ($\gg\xi$) in the SANS regime and in SLS regimes, respectively, and the scattering intensity is given by

$$I(q) = \frac{A_{SLS}}{1+\Xi^2 q^2} + \frac{A_{SANS}}{1+\xi^2 q^2} \quad \text{(another OZ function)} \tag{9}$$

If this is the case, then Tetra-PEG gels are a one-phase system that has bimodal concentration fluctuations in submicrometers and a few tens of angstroms. We speculate that the inhomogeneities characterized by ξ correspond to the distance between polymer-poor regions originating from imperfect cross-end-coupling reaction. Further investigations to elucidate this conjecture are in progress.

5. Conclusions

The structure of Tetra-PEG gels was investigated by SANS as well as SLS. The following facts are disclosed: (1) The TAPEG macromer solutions, consisting of tetra-arm polymer chains, are not interpenetrable because of the presence of end groups, and the individual chains behave as hard spheres. Therefore, the radius of gyration, R_g, scales with $\phi_0^{-1/3}$. (2) The structure factors of both as-prepared and swollen gels in the SANS regime can be represented by Ornstein–Zernike-type scattering functions and be superimposed to single master curves, irrespective of the molecular weight. (3) No inhomogeneities appeared even by swelling. (4) However, in the SLS regime, a steep upturn was observed in SANS curves in as-prepared Tetra-PEG gels, indicating the presence of PEG chain clusters or defects. A master-curve relationship holds also in the SLS regime for a gel having the same molecular weight, indicating a self-similar network structure in Tetra-PEG gels. (5) The upturn in scattering intensity is assigned to be a clustered structure, as is often observed in PEG in water, network defects, or both. The upturn is suppressed by increasing M_w because of the formation of more regular network structures with less inhomogeneities. It is concluded that Tetra-PEG gels have no noticeable entanglements but have self-similar structures with respect to M_w and form ideal tetrafunctional polymer networks provided that M_w is high enough ($\sim 40 \times 10^3$).

Acknowledgment. This work was partially supported by the Ministry of Education, Science, Sports and Culture, Japan (Grants-in-Aid for Scientific Research (A), 2006-2008, no. 18205025, and for Scientific Research on Priority Areas, 2006-2010, no. 18068004). The SANS experiment was performed with the approval of the Institute for Solid State Physics, The University of Tokyo, at Japan Atomic Energy Agency, Tokai, Japan no. 8615. We are grateful to Dr. B. Hanmouda for valuable discussion and supply of SANS data.

References and Notes

(1) Stein, R. S. *J. Polym. Sci.* **1969**, *B7*, 657–660.
(2) Pines, E.; Prins, W. *J. Polym. Sci., Polym. Phys. Ed.* **1972**, *B10*, 719–724.
(3) Candau, S.; Bastide, J.; Delsanti, M. *Adv. Polym. Sci.* **1982**, *44*, 27.
(4) Panyukov, S.; Rabin, Y. *Macromolecules* **1996**, *29*, 7960.
(5) Bastide, J.; Candau, S. J. Structure of Gels as Investigated by Means of Static Scattering Techniques (Chapter 9). In *The Physical Properties of Polymer Gels*; Addad, J. P. C., Ed.; John Wiley: New York, 1996; p 143.
(6) Shibayama, M. *Macromol. Chem. Phys.* **1998**, *199*, 1–30.
(7) Panyukov, S.; Rabin, Y. *Phys. Rep.* **1996**, *269*, 1–132.
(8) Flory, P. J.; Rehner, J.Jr. *J. Chem. Phys.* **1943**, *11*, 521.
(9) Treloar, L. R. G. *The Physics of Rubber Elasticity*; Clarendon Press: Oxford, U.K., 1975.
(10) Mallam, S.; Horkay, F.; Hecht, A. M.; Geissler, E. *Macromolecules* **1989**, *22*, 3356.
(11) Pusey, P. N.; van Megen, W. *Physica A* **1989**, *157*, 705–741.
(12) Joosten, J. G. H.; Gelade, E. T. F.; Pusey, P. N. *Phys. Rev. A* **1990**, *42*, 2161–2175.
(13) Shibayama, M.; Norisuye, T. *Bull. Chem. Soc. Jpn.* **2002**, *75*, 641–659.
(14) Zhao, Y.; Zhang, G.; Wu, C. *Macromolecules* **2001**, *34*, 7804–7808.
(15) Ikkai, F.; Shibayama, M. *Phys. Rev. Lett.* **1999**, *82*, 4946–4949.
(16) Shibayama, M.; Tsujimoto, M.; Ikkai, F. *Macromolecules* **2000**, *33*, 7868–7876.
(17) Shibayama, M.; Takata, S.; Norisuye, T. *Physica A* **1998**, *249*, 245–252.
(18) Mark, J. E.; Erman, B. *Rubberlike Elasticity: A Molecular Primer*; Wiley: New York, 1988.

(19) Mark, J. E.; Sullivan, J. L. *J. Chem. Phys.* **1977**, *66*, 1006–1011.
(20) Jong, L.; Stein, R. S. *Macromolecules* **1991**, *24*, 2323–2329.
(21) Sullivan, J. L.; Mark, J. E.; Hampton, P. G.; Cohen, R. E. *J. Chem. Phys.* **1978**, *68*, 2010–2012.
(22) Mark, J. E.; Rahalkar, R. R.; Sullivan, J. L. *J. Chem. Phys.* **1979**, *70*, 1794–1797.
(23) Llorente, M. A.; Mark, J. E. *J. Chem. Phys.* **1979**, *71*, 682–689.
(24) Geissler, E.; Horkay, F.; Hecht, A. M.; Rochas, C.; Lindner, P.; Bourgaux, C.; Couarraze, G. *Polymer* **1997**, *38*, 15.
(25) Mendes, E.; Hakiki, A.; Herz, J.; Boué, F.; Bastide, J. *Macromolecules* **2004**, *37*, 2643–2649.
(26) Sukumaran, S. K.; Beaucage, G.; Mark, J. E.; Viers, B. *Eur. Phys. J. E* **2005**, *18*, 29–36.
(27) Sakai, T.; Matsunaga, T.; Yamamoto, Y.; Ito, C.; Yoshida, R.; Suzuki, S.; Sasaki, N.; Shibayama, M.; Chung, U. *Macromoleules* **2008**, *41*, 5379–5384.
(28) Matsunaga, T.; Sakai, T.; Akagi, Y.; Chung, U.; Shibayama, M. *Macromolecules* **2009**, *42*, 1344–1351.
(29) Benoit, H. *J. Polym. Sci.* **1953**, *11*, 507–510.
(30) Richter, D.; Farago, B.; Huang, J. S.; Fetters, L. J.; Ewen, B. *Macromoleules* **1989**, *22*, 468–472.
(31) de Gennes, P. G. *Scaling Concepts in Polymer Physics*; Cornell University: Ithaca, NY, 1979.
(32) Ornstein, L. S.; Zernike, F. *Proc. Acad. Sci. Amsterdam* **1914**, *17*, 793.
(33) Okabe, S.; Karino, T.; Nagao, M.; Watanabe, S.; Shibayama, M. *Nucl. Instrum. Methods Phys. Res., Sect. A* **2007**, *572*, 853–858.
(34) Okabe, S.; Nagao, M.; Karino, T.; Watanabe, S.; Adachi, T.; Shimizu, H.; Shibayama, M. *J. Appl. Crystallogr.* **2005**, *38*, 1035–1037.
(35) (a) Shibayama, M.; Nagao, M.; Okabe, S.; Karino, T. *J. Phys. Soc. Jpn.* **2005**, *74*, 2728–2736. (b) Shibayama, M.; Matsunaga, T.; Nagao, M. *J. Appl. Crystallogr.* **2009**, *42*, 621–628.
(36) Lutolf, M. P.; Hubbell, J. A. *Biomacromolecules* **2003**, *4*, 713–722.
(37) Bastide, J.; Leibler, L. *Macromolecules* **1988**, *21*, 2647.
(38) Mendes, E. J.; Lindner, P.; Buzier, M.; Boue, F.; Bastide, J. *Phys. Rev. Lett.* **1991**, *66*, 1595.
(39) Mendes, E.; Girard, B.; Picot, C.; Buzier, M.; Boue, F.; Bastide, J. *Macromolecules* **1993**, *26*, 6873.
(40) Mendes, E.; Oeser, R.; Hayes, C.; Boue, F.; Bastide, J. *Macromolecules* **1996**, *29*, 5574.
(41) Shibayama, M.; Shirotani, Y.; Hirose, H.; Nomura, S. *Macromolecules* **1997**, *30* (23), 7307.
(42) Shibayama, M.; Shirotani, Y.; Shiwa, Y. *J. Chem. Phys.* **2000**, *112*, 442–449.
(43) Hammouda, B.; Ho, D.; Kline, S. *Macromolecules* **2002**, *35*, 8578–8585.
(44) Zhou, P.; Brown, W. *Macromolecules* **1990**, *23*, 1131–1139.
(45) Hammouda, B.; Ho, D. L.; Kline, S. *Macromolecules* **2004**, *37*, 6932–6937.
(46) Polik, W. F.; Burchard, W. *Macromolecules* **1983**, *16*, 978–982.
(47) Wu, W.; Shibayama, M.; Roy, S.; Kurokawa, H.; Coyen, L. D.; Nomura, S.; Stein, R. S. *Macromolecules* **1990**, *23*, 2245–2251.
(48) Onuki, A. *J. Phys. II* **1992**, *2*, 45–61.
(49) Bouchaud, E.; Delsanti, M.; Adam, M.; Daoud, M.; Durand, D. *J. Phys.* (*Paris*) **1986**, *47*, 1273–1277.
(50) Adam, M.; Delsanti, M.; Munch, J. P.; Durand, D. *J. Phys.* (*Paris*) **1987**, *48*, 1809–1818.
(51) Adam, M.; Lairez, D. Sol-Gel Transition. In *Physical Properties of Polymeric Gels*; Cohen Addad, J. P., Ed.; John Wiley & Sons: New York, 1996; p 87.